Electron microscopy and diffraction study of phospholipid monolayers transferred from water to solid substrates

A. Fischer, E. Sackmann

HAL Id: jpa-00209782
https://hal.science/jpa-00209782

Submitted on 4 Feb 2008

Electron microscopy and diffraction study of phospholipid monolayers transferred from water to solid substrates

A. Fischer and E. Sackmann

Technical University of Munich, Physics Department (E22), D-8046 Garching, F.R.G.

Résumé. — Des films monomoléculaires de phospholipides (phosphatidylcholine et acide phosphatidique) et acide arachidique ont été transférés d'une interface air/eau sur des substrats hydrophiles transparents aux électrons tels que 1) films de carbone, 2) couches cristallines de graphite oxydé, 3) feuilles de Formvar recouvertes de SiO_2. Ces films ont été étudiés en microscopie électronique par transmission, soit conventionnelle soit à balayage en fond noir annulaire, et aussi en diffraction électronique. Une coloration positive à l'acétate d'uranyl, accompagnée d'un ombrage au platine sous incidence rasante, a été effectuée. Cette dernière méthode a permis de mesurer l'épaisseur des couches lipidiques transférées avec une précision de 10 %. On a observé pour la première fois des monocouches dans le mode en transmission sous des grandissements variables de × 2 000 à 50 000. Des schémas de diffraction électronique ont été enregistrés à partir de films qui, dans tous les cas, ont été caractérisés simultanément par microscopie conventionnelle.

Nous avons comparé la structure des monocouches déposées à partir de 1) l'état solide complètement condensé, 2) l'état intermédiaire, 3) l'état fluide expansé, et 4) la région où se place la principale transition de phase. Nous montrons que l'état de la monocouche à l'interface air/eau est au moins partiellement préservé lors du dépôt.

Dans l'état complètement condensé, les acides gras et phosphatidiques forment des monocouches macroscopiquement continues. Les chaînes forment un réseau triangulaire (paramètre $d_{100} = 4,2$ Å ; surface par molécule 40 Å^2) et sont orientées perpendiculairement à la surface. Les phosphatidylcholines déposées présentent un réseau de fractures larges de 100 Å en toile d'araignée. Ce lipide est incliné d'environ 20 degrés par rapport à la normale à la monocouche et forme un réseau orthorhombique aussi bien à l'interface air/eau que sur le substrat. Une comparaison des largeurs radiales des raies de diffraction de la monocouche avec celles des substrats de graphite oxydé montre que la phase à haute pression de tous les lipides ne présente pas de véritable ordre à longue distance des chaînes.

Dans la région de pression intermédiaire — également appelée région fluide condensé —, le film consiste en une accumulation de petites plaques d'environ 1 µm de diamètre qui — du moins selon la figure de diffraction électronique — sont certainement cristallisées sur le substrat. La grande taille des plaquettes montre que le cœur de la monocouche est également cristallisé à la surface de l'eau tandis qu'une petite partie peut rester à l'état fluide. La viscosité de type liquide de la phase intermédiaire est attribuée à la faible résistance au cisaillement de l'agrégat de plaquettes. La transition du type second ordre vers l'état complètement cristallisé est attribuée à l'apparition des plaquettes.

Dans la région où se produit la transition de phase principale, nous montrons que la monocouche est formée de domaines fluides et cristallisés d'environ 100 Å de diamètre. La pente finie de l'isotherme à la transition n'est donc pas un artefact mais résulte de la taille finie des unités individuelles qui transitent de façon coopérative. Ceci confirme notre précédente interprétation ainsi qu'une récente étude par la méthode de Monte-Carlo de la nature de la transition de phase due à Georgallas et Pink, *Can. J. Phys.* **60** (1982) 1678.

Abstract. — Monomolecular films of phospholipids (phosphatidylcholines and phosphatidicacids) and arachidonic-acid were transferred from air/water interface onto electron transparent hydrophilic substrates such as 1) carbon films, 2) crystalline graphite-oxide layers, 3) SiO_2-covered Formvar foils and were studied by conventional transmission electron microscopy (TEM), by scanning transmission STEM in the darkfield mode and by electron diffraction. Positive staining with uranylacetate and platinum shadowing, using a low angle of incidence, was applied. The latter allowed measurements of the thickness of the transferred lipid layers to an accuracy of 10 %. Imaging of monolayers in the transmission mode at magnifications of × 2 000-50 000 was achieved for the first time. Electron diffraction patterns were taken from layers which in all cases have been characterized simultaneously by conventional EM.

The structure of monolayers transferred 1) from the completely condensed solid state, 2) from the intermediate state, 3) from the expanded (fluid) state and 4) from the region of the main phase transition are compared. Evidence is provided that the state of the monolayer on the air-water interface is at least partially preserved upon transfer.

In the completely condensed state macroscopically continuous monolayers are formed by fatty acids and phosphatidic acid. The chains form a triangular lattice (lattice constant d_{100} = 4.2 Å ; area per molecule 40 Å^2) and are oriented normal to the surface. The transferred phosphatidylcholines exhibit a spider's web of elongated 100 Å wide cracks. This lipid is tilted with respect to the monolayer normal by about 20 degrees and forms and orthorhombic lattice both at the air/water interface and on substrate. A comparison of the radial widths of the electron diffractions of the monolayer with that of graphite oxide substrates provides evidence that the high pressure phase of all lipids do not exhibit a true long-range order of the chains.

In the intermediate pressure region — also called fluid condensed region — the film consists of an accumulation of platelets of about 1 μm diameter which according to electron diffraction — are certainly crystalline on the substrate. The large size of the platelets shows that the bulk of the monolayer is also crystalline on the water surface, while a small fraction may still be in the fluid state. The fluid-like viscosity of the intermediate phase is attributed to the low shearing strength of the accumulation of platelets. The 2nd order like transition into the completely condensed crystalline phase is attributed to the merging of the platelets.

Evidence is provided that in the region of main phase transition the monolayer consists of fluid and crystalline domains of some 100 Å diameter. The finite slope of the isotherm at the main transition is thus not an artefact but is due to the finite size of the cooperative unit undergoing a simultaneous transition. This confirms our previous interpretation and a recent Monte-Carlo study of the nature of the phase transition by Georgallas and Pink (*Can. J. Phys.* **60** (1982) 1678).

1. Introduction.

Monolayers of phospholipids are gaining growing interest for several reasons : they may be applied in membrane research (1) in order to study certain physical properties of membranes [1], (2) to prepare black lipid films of the Montal type [2] and (3) to immobilize cells [3]. From a physical point of view monolayers are interesting because they are at the borderline between two- and three-dimensional systems [4, 5]. Finally, phospholipid monolayers are becoming of practical interest as insulating layers on semiconductors [6] or to modify solid surfaces for applications in integrated optics [7]. The range of technological applications of monolayers is greatly enlarged by the recent success in preparing a variety of polymerizable lipids [8, 9].

From both a scientific and a technical standpoint the structural phase transitions of the lipid monolayers are of central interest. In a previous study of the polymorphism of phospholipid monolayers [1] we reported three transitions above the millidyne pressure region which are indicated in the schematic phase diagram shown in figure 1. Besides the well known transition at π_m associated with a large change in molecular area [1, 4, 10] there are two additional transitions located at (π_c) and (π_f). These have the characteristic features of a 2nd order transition since they exhibit breaks in the pressure (and/or temperature) dependencies of the compressibility and the thermal expansion coefficient, respectively [1]. The transition at π_f was attributed to a fluid-fluid phase change. However, a more recent study [11] provided evidence that it could also correspond to a change from a homogeneous to a heterogeneous fluid phase, reminiscent of a two-dimensional vapour. The π_c transition was tentatively interpreted in terms of a change from a tilted solid to a non-tilted solid phase. An alternative explanation is given by Cadenhead
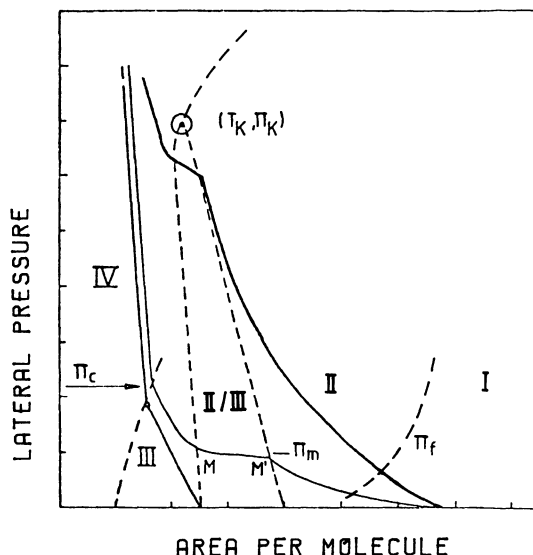

AREA PER MOLECULE

Fig. 1. — Schematic representation of pressure area phase diagram of phospholipid monolayers showing the different phases and coexistence regions. The drawn lines are representative isotherms while the broken lines indicate phase transitions or boundaries of coexistence regions as suggested by a previous film balance study [1]. π_c and π_f denote a solid-solid and a fluid-fluid transition, respectively and (π_k, T_k) is a tricritical point. Region IV corresponds to the completely compressed solid state while region III was attributed to a tilted solid phase. I and II denote the two fluid phases separated by the transition at π_f and II/III is the fluid-solid coexistence region.

et al. [4] or Phillips *et al.* [10] on the basis of the older work of Adam. These authors attributed the (main) transition at π_m to a change from a liquid expanded to a liquid condensed phase. In this picture the symmetry-breaking fluid-to-solid transition would have to be attributed to the 2nd-order like (III → IV) phase change at π_c. Another interpretation was given by

Tscharner and McConnel [3] who postulated that within region III of figure 1 one deals with a heterogeneous state of a coexisting fluid and a solid phase.

In order to gain more insight into the nature of the condensed states we performed a transmission electron microscopy study of monolayers transferred from the air/water interface (1) to carbon films (2) to crystalline layers of graphite oxide and (3) to Formvar foils covered with SiO_2.

A variety of techniques was applied. These included (1) electron diffraction, (2) phase contrast transmission electron microscopy and (3) the scanning transmission technique (STEM). By shadowing under flat angles of incidence of 15°, the layer thickness could be determined to an accuracy of about 10 % which allowed to distinguish unambiguously between monolayers and multilayers.

2. Experimental methods.

2.1 METHOD OF MONOLAYER TRANSFER. — The film balance as well as the method of film spreading was described previously [1]. The lipids, DMPC, DPPC, DSPC, DPPA and C20 ([1]), were products of Sigma and were used without additional purification.

For all substrates the graphite oxide layers, the carbon films and the SiO_2-covered Formvar foils electron microscope (EM-)grids were used as a support. The graphite oxide was a gift of Dr. Formanek from LMU Munich and is supposed to provide a hydrophilic surface [12]. The carbon layers were prepared as follows [13] : a carbon film of 100-200 Å thickness was deposited onto freshly cleaved mica sheets by evapouration in a Balzers BAF400D freeze fracture device at a pressure of 5×10^{-6} mbar. Then the film was transferred onto a water (millipore purified) surface by floating. The floating carbon film was then transferred to an EM-grid which was located just beneath the water surface. This was achieved by slowly lowering the water level. The following different techniques were applied in order to obtain a hydrophilic surface of the carbon films ; (1) aging in air for some days (2) treatment by a glow discharge in an oxygen atmosphere and (3) dipping into 1 % by weight solutions of alcian blue and ethidium bromide [14]. Secondary ion mass spectroscopy shows that the treatment in the glow discharge leads to an enhancement of the surface concentration of aluminium and silicon.

Formvar coated grids on microscope slides were prepared as described in [13]. In order to obtain a hydrophilic surface a 5 Å thick layer of SiO_2 was deposited on the foil. Contact angle measurements

showed that the surface was indeed hydrophilic. Due to the small electrical and thermal conductivity the samples could only be observed by darkfield STEM.

The transfer of the lipid monolayer from the air/water interface onto the substrates was performed as follows : the microscope grids carrying carbon films or graphite oxide as substrates were pressed onto filter paper with a pair of tweezers. This whole support system was dipped into the water bath of the film balance. Now, the film was spread as described in reference [1] and the lateral pressure was set to a preselected value. The support was then lifted through the monolayer at a constant speed of 3 mm/min. Since both the filter paper and the substrate are hydrophilic only one monolayer is transferred. Finally the sample was dried on a stainless steel net in order to remove residual water remaining between the meshes of the electron microscope grid. The procedure was somewhat different for the SiO_2 covered Formvar foils. Here the foils extended over the grid as well as over the cover glass. The monolayer was deposited on the whole foil as described above. After this the foil was removed from the glass support together with the grid. The advantage of this procedure is that boundary effects are minimized.

2.2 STAINING AND SHADOWING. — Both a positive staining technique and platinum shadowing were used. For positive staining uranyl-acetate was added to the aqueous phase of the film balance before spreading of the film. The final salt concentration was 5×10^{-4} m. Before use, the uranyl acetate was filtered by a Gelman filter. The salt leads to a considerable shift of the main phase transition to lower transition pressures π_m but the shape of the isotherms is not significantly affected by the salt. Platinum shadowing is performed in a Balzers BAF400D freeze etching device under a very flat angle of incidence of $\alpha = 15°$. The thickness, d, of the lipid layer can thus be determined from the width, l, of the shadow according to

$$d = 1 \tan \alpha \approx 1/4 .$$

2.3 ELECTRON MICROSCOPY TECHNIQUES. — The electron microscopy study was performed with a Phillips EM400T microscope equipped with a scanning transmission (STEM) system. A conventional tungsten hair-pin filament was used limiting the resolution to about 50 Å. The phase contrast TEM was achieved in the conventional way by using very coherent illumination and by defocusing. The contrast depends on the degree of defocusing. In our experiments the following settings were used : (i) « Magnification Mode » : × 2 800 ; condensor aperture 10 μm ; defocus 500 nm ; (ii) so-called « Low Magnification Mode » : × 2 200 ; condensor aperature 50 μm ; defocus 200 μm.

At high magnification the darkfield technique in the TEM mode is not efficient since only parts of the scattered electrons are used for the image reconstruction. Therefore the dark field STEM technique was

---

([1]) The following abbreviations are used :
dipalmitoylphosphatidylcholine : DPPC
dimyristoylphosphatidylcholine : DMPC
distearoylphosphatidylcholine   : DSPC
dipalmitoylphosphatidic acid   : DPPA
arachidonic acid   : C20.

applied [15]. In this mode the sample is scanned with a beam of 50 Å diameter. An annular dark field detector with an inner diameter of 2 mm and an outer diameter of 22 mm collects elastically scattered electrons. The primary beam going through the inner aperture is collected by an additional disk-shaped inner bright field detector. Provided that only the scattered electrons are used for image reconstruction, a contrast higher than with the other techniques is achieved which is sufficient to detect single monolayers.

For the electron diffraction the Rieke selected area technique was applied using coherent beam illumination [16]. The illuminated area on the specimen had a diameter of 1-3 µm. A 10 µm condensor aperture was used. The diffraction pattern in the back focal plane of the objective lens was magnified on the screen and on the camera. For the calibration of the camera length, a 50 Å gold layer is deposited on a certain area of the specimen. A more elegant technique of calibration is based on the use of crystalline graphite oxide substrates which provide an internal standard.

To minimize radiation damage the Low Dose unit of the EM400 was used. In this mode the necessary adjustments of the lenses are first made by monitoring the diffraction pattern of a certain area of the monolayer. The pattern which is actually recorded is taken from a new somewhat adjacent area since the Low Dose unit allows one to switch between different areas without a loss of the image or diffraction spot sharpness. After completion of the diffraction experiments, a normal electron micrograph of the same area was taken in order to characterize the monolayer region from which the diffraction pattern has been taken. For further evaluation of the microscopic structure, the previously studied specimen was subsequently shadowed with platinum in the Balzer's BAF400D device and is then once again observed in the electron microscope at high magnification. For image recording Kodak 4489 and for the diffraction experiments Kodak SO 163 plates were used.

3. Experimental results.

3.1 ARACHIDONIC ACID LAYERS. — A typical low-temperature isotherm is given in figure 2a. The horizontal line at $\pi = 0$ which is observed at low density goes over into a curve which consists of two nearly straight line regions which intercept at π_c. This corresponds to a direct transition from the expanded gaseous state to the condensed phase III and to a III → IV transition at π_c. Figures 2b and 2c show electron micrographs of films transferred at a pressure above ($\pi = 40$ mN/m) and below ($\pi = 10$ mN/m) the transition pressure π_c. The samples were both positively stained and platinum shadowed under an angle of 15°.

At the higher pressure a continuous layer extending over some 10 µm is observed which exhibits small holes of an average diameter of about 500 Å. The holes comprise about 5 % of the total layer area. At low

pressure (Fig. 2c) one observes only irregularly shaped patches of lipid layer which are well separated. A similar type of platelet structure was reported previously by Ries and Walker [18]. Both the holes of figure 2b and the patches of figure 2c exhibit bright and dark rims. The width of the shadows is about 100 Å from which one estimates a thickness of the layers of 30 ± 5 Å. This corresponds rather well to the thickness of one monolayer. The shadowing technique is thus well suited to distinguish between mono- and multilayers.

Figure 2d shows an electron diffraction pattern of the C20 monolayer transferred at 30 mN/m. It shows three hexagonal arrays of reflections. One of these arrays is rotated with respect to the other two by 30°. The ratio of the distances is $1 : \sqrt{3} : 2$. Obviously the chains are forming a triangular lattice as shown in figure 3. The intensity decreases sharply with increasing scattering angle so that the 2nd order 200-reflections are seldom visible.

In a separate experiment the absolute value of the scattering angle of the innermost reflections has been determined by comparison with the diffraction pattern of the graphite oxide layer. A value of $d_{100} = 4.2$ Å was obtained.

3.2 DIPALMITOYLPHOSPHATIDIC ACID (DPPA). — The isotherm of this lipid at 20 °C looks quite similar to that of arachidonic acid. In figure 4a a micrograph of the film deposited from a high pressure (30 mN/m) is shown. A continuous monolayer at least over distances of some 10 µm is observed which exhibits broad cracks free of lipid (black areas in Fig. 4a).

Figure 4b shows the monolayer transferred from a pressure below π_c. One observes a mosaic-like accumulation of platelets which are connected by grainy material (cf. Fig. 4b left side). Both have a thickness corresponding to that of a monolayer. At the right side a platelet is shown at higher magnification which was achieved by application of the TEM technique. Obviously, the seemingly continuous platelets exhibit small elongated holes of about 100×500 Å^2 diameter.

Note that the monolayer in figure 4a was only stained by uranylacetate. By application of the STEM system of the EM400T it is obviously possible to achieve an extremely high contrast. A diffraction pattern of the monolayer deposited on graphite oxide from a high pressure (30 mN/m) is shown in figure 5. We obtained a ring-like pattern for all preparations of this lipid. Occasionally a weak hexagon-structure is superimposed.

3.3 MONOLAYERS OF DIACYL-PHOSPHATIDYLCHO-LINES. — The staining of lecithin monolayers with uranyl acetate leads to a remarkable shift in the transition pressure π_m while the form of the isotherms remains essentially unchanged (cf. Fig. 6). At the salt concentration of 5×10^{-4} M used in our experiments, the critical points are shifted to lower pressures by about 10 mN/m. Note that at that salt concentration
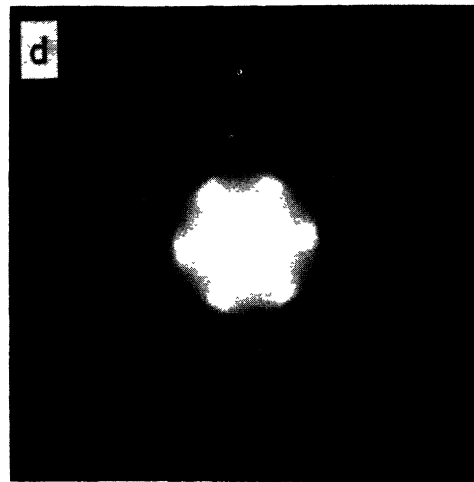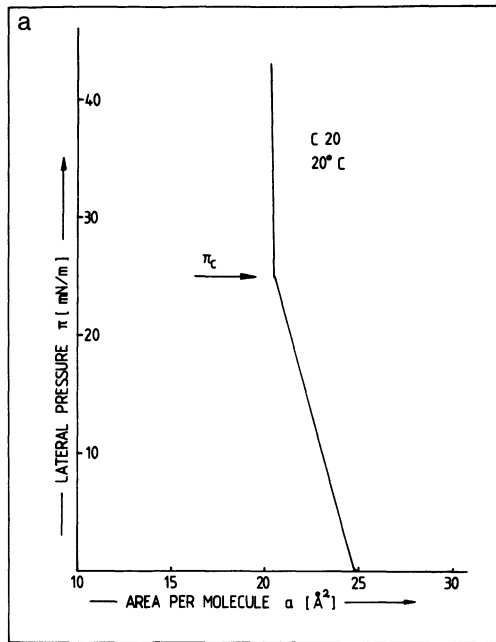
Fig. 2. — a) Isotherm of arachidonic acid (C20) taken at 20 ℃. The form is typical for a direct transition from an expanded — most probably gaseous — phase to state III and subsequently to state IV.

b) Micrograph C20-monolayer transferred from on carbon 40 mN/m after staining and platinum shadowing. The shadowing direction is indicated by arrow. Bar 0.5 μm.

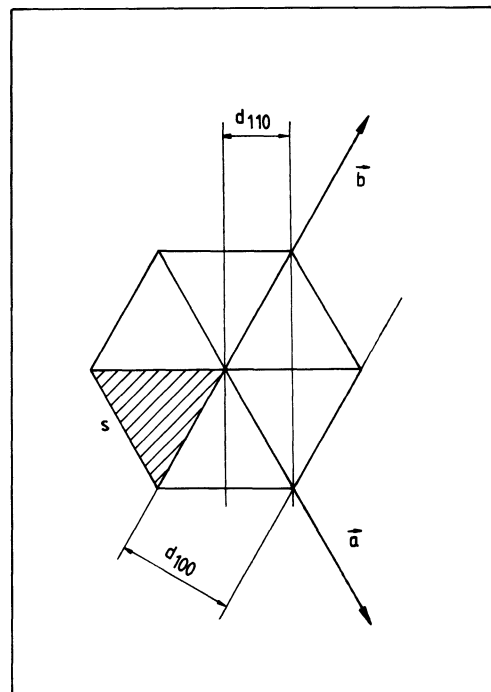c) Micrograph of monolayer transferred at 10 mN/m. Arrow : shadowing direction. Bar 0.1 μm.

d) Electron diffraction pattern of monolayer transferred onto carbon film at a pressure of 30 mN/m. The diffuse rings are from the carbon support film.
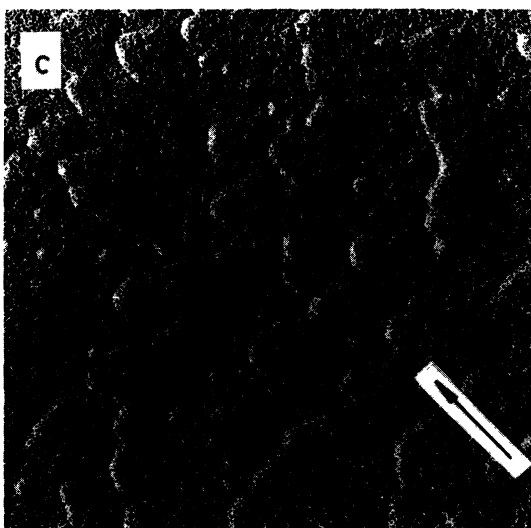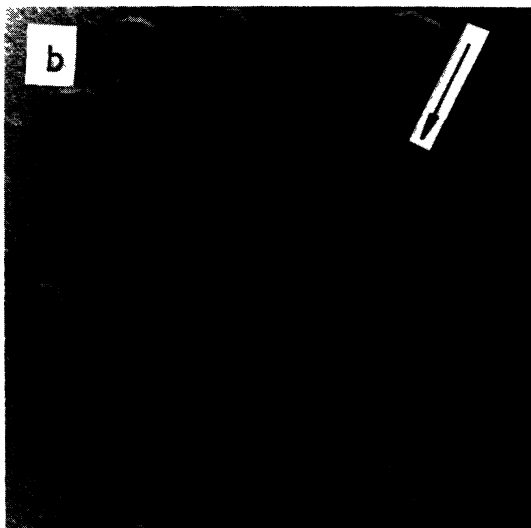

Fig. 3. — Lattice of hydrocarbon chains of arachidonic acid or phospholipid molecules. The chains are oriented in a direction normal to the plane of the bilayer and are forming a triangular lattice. The lattice constants are $d_{100} = \frac{s}{2}\sqrt{3}$ and $d_{110} = \frac{s}{2}$, where s is the interchain distance.
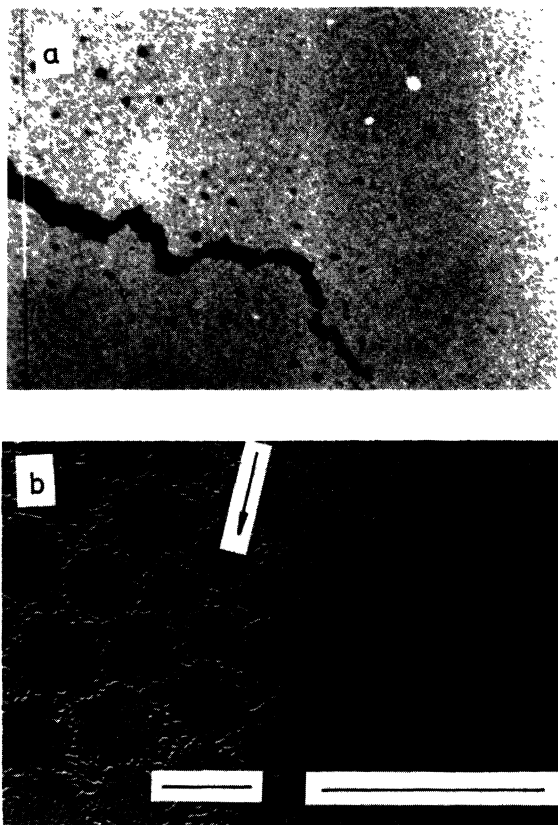
Fig. 4. — a) Micrograph of DPPA monolayer transferred from π = 30 mN/m on carbon film. The monolayer is only stained with uranylacetate and is observed by the darkfield STEM technique. Bar 0.5 μm.

b) Electron micrograph of dipalmitoylphosphatidicacid (DPPA) transferred on carbon film from π = 5 mN/m. *Left side* : picture of stained and shadowed sample taken by dark field STEM.

Right side : platelet as observed on left side taken by conventional TEM higher magnification. Note the very small holes within the platelets which are not visible at left side. The shadowing direction is the same for both pictures. Bar 0.5 μm.
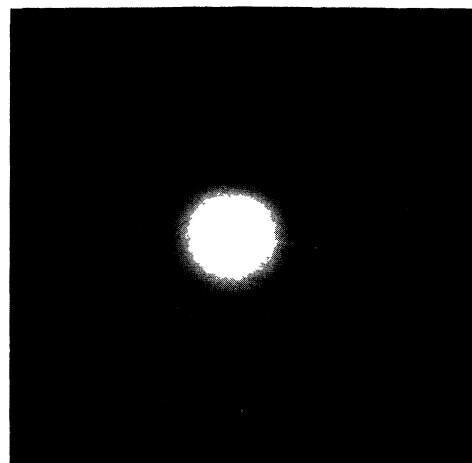

Fig. 5. — Electron diffraction pattern of DPPA monolayer deposited onto graphite oxide crystal platelet. The ring-like pattern with superimposed hexagon is due to lipid. The graphite oxide yields sharp spots.
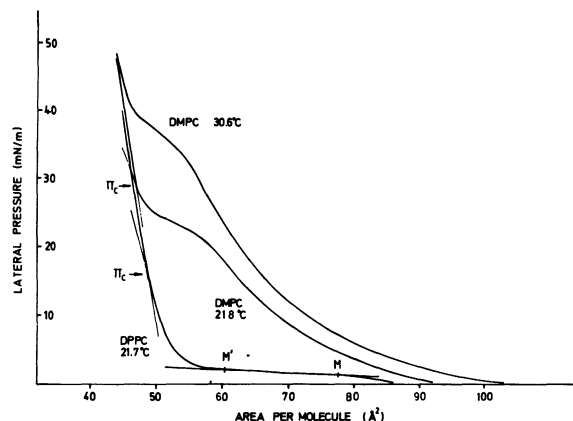

Fig. 6. — Characteristic isotherms of phospholipid monolayers. The data correspond to DMPC at 30.6 °C, to DPPC at 21.7 °C and DMPC at 21.8 °C on 5 × 10^{-4} M uranyl acetate solution. Clearly visible is the transition at π_m which extends over the straight line region between MM' and the second order-like transition at π_c indicated by arrows.

the main transition of the lecithin vesicles is shifted by about 5 °C to higher temperatures.

The texture of the transferred film may depend on the pressure from which the film is deposited [17, 18]. This may create difficulties if one wants to compare films at the different states II-IV (cf. Fig. 1). In order to have the same standard conditions we transferred all films at the same high pressure of 30-40 mN/m. We therefore varied the type of lipid as well as the temperature in order to achieve this goal. We used (1) DPPC at 18 °C as a representative of the state IV, (2) DMPC at 22 °C as a prototype of a monolayer in state III (3) DMPC at 23 °C as a monolayer in the coexistence region II/III and (4) DMPC at 32 °C as an example of the fluid phase (II).

Figures 7 et 8 show the electron micrographs of the lecithin monolayers transferred from the different

states. All the monolayers were transferred after compression from zero pressure to 30 mN/m. The following characteristic features are observed :

1) If transferred from state IV (Fig. 7a) the monolayer is continuous and completely devoid of holes within areas of diameter of some μm while cracks of some 100 Å width run across the monolayer in two nearly perpendicular directions. Thus roughly hexagonally shaped platelets are formed. The overal structure of this spider's web of cracks will be more clearly shown in figure 11.

2) In the state III (Fig. 7b) the web of cracks is still visible. In addition, the platelets (of about 1 μm crosssection) exhibit now small holes of some 100 Å diameter.

Fig. 8. — a) Darkfield STEM of DMPC transferred at 23 °C and 30 mN/m corresponding to the coexistence region. Technique and substrate as in figure 7. Bar 0.5 μm.

b) Darkfield STEM of DMPC transferred from the fluid phase I (= 30 mN/m; 32 °C) : Technique and substrate as in figure 7. Bar 0.5 μm.
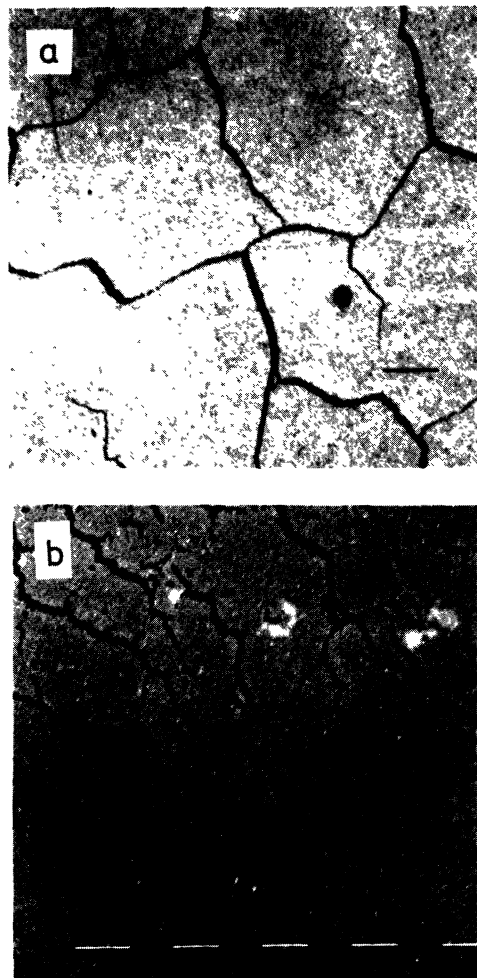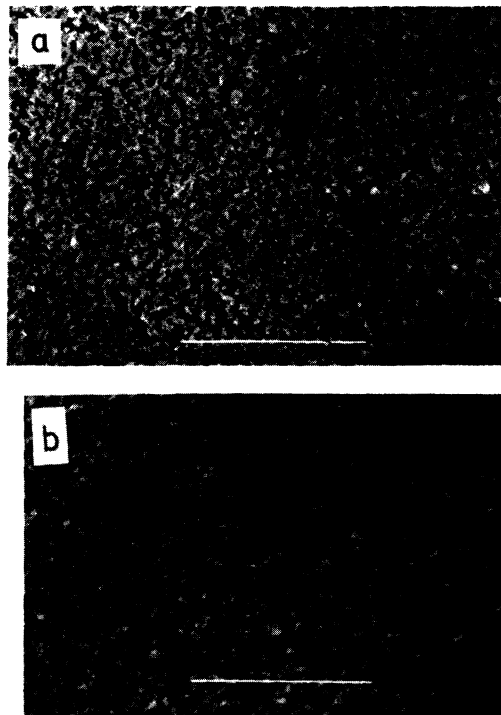
Fig. 7. — a) Dark field STEM micrograph of DPPC transferred from the completely condensed crystalline state IV (30 mN/m, 20 °C) onto SiO₂ covered Formvar film. The completely dark spots correspond to holes in the Formvar foil. The film was only stained with uranyl acetate. Bar 0.5 μm.

b) Dark field STEM picture of DMPC transferred from state III (30 mN/m 20 °C). Technique and substrate as above. Bar 0.5 μm.

3) In the coexistence region II/III (Fig. 8a) the monolayer has completely broken up into small islands of about 500 Å diameter. About 20 % of the total surface appears to be uncovered.

4) If the film is transferred from the fluid phase II even smaller islands of about 200 Å are formed. A higher fraction of the substrate surface is uncovered.

Figure 9 shows the electron diffraction pattern obtained from the DPPC monolayer transferred from the completely condensed state IV. A hexagonal diffraction pattern is observed together with a weak ring. This shows that the transferred monolayer forms two-dimensional crystals with diameters of some 10 μm. It should be noted that after each diffraction experiment the covered area on the substrate was observed by the conventional electron microscopy.
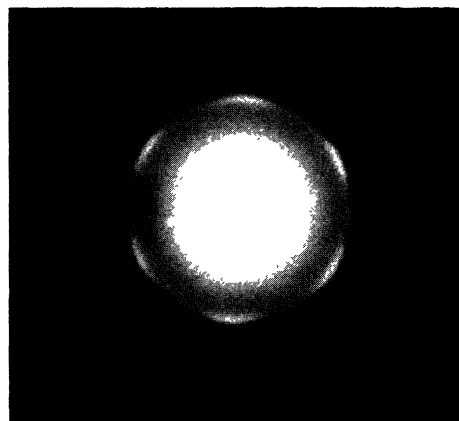

Fig. 9. — Electron diffraction pattern of DPPC monolayer on carbon in state IV.

The monolayers transferred from states III and II as well as the II/III coexistence region show also relatively sharp diffraction rings. The intensity is, however, much lower than that of figure 9.

3.4 DENSITOMETRIC EVALUATION OF DIFFRACTION PATTERN. — For a quantitative evaluation of the electron diffraction patterns it is necessary to control the divergence of the electron beam at the specimen and to

minimize line broadening caused by the magnification of the diffraction pattern. This problem was solved by using graphite oxide as a substrate. This crystalline material yields sharp diffraction spots and thus allows us to control the quality of the imaging. Simultaneously it gives an inner standard for determining absolute values of the lattice constant of the monolayer as well as the width of the diffractions.

The results of the densitometric evaluation are summarized in figure 10 and table I. DPPA and C20 exhibit a single 100 reflection. Compared to the graphite oxide substrate the bands are considerably broadened. The value of the lattice constant $d_{100} = 4.3 \pm 0.1$ Å for DPPA is by about 0.1 Å larger than that of C20 and by about 0.2 Å larger than the values obtained by X-ray diffraction for the crystalline $P_{\beta'}$-phase of fully hydrated phosphatidylcholines [19]. The 100 reflections of DMPC are very broad and seem to consist of two bands with maxima at 4.3 Å and 4.5 Å. The average value of the lattice constant is $d_{100} = 4.4$ Å. The areas per chain calculated from the lattice constants agree well with the film balance data (cf. Table I). For the case of DMPC the average value of $d_{100} = 4.4$ Å has been taken in order to determine the area per chain in table I.

4. Discussion.

The main aim of the present work was (1) to evaluate the potentiality of the electron microscopy to study the microstructure and molecular organization of phospholipid monolayers and (2) to try to transfer certain monolayer phases from the air/water interface onto thin solid substrates so that they could be observed by transmission electron microscopy.

4.1 STRUCTURE OF THE CONDENSED STATES.

4.1.1 *High pressure phase IV.* — The transfer of continuous films on solid substrates is only possible from high pressures : $\pi > \pi_c$. The diffraction experiments show that under these conditions two-dimensional single crystals may be obtained for the fatty acid (C20). The lecithins form two-dimensional crystals which are broken up into domains, the crystal planes of which are nearly parallel. The radial widths of the diffractions for C20 and DPPA are considerably smaller than for the lecithines. In the latter case the diffractions seem to consist of two peaks corresponding to lattice constants of $d_{100} = 4.3$ Å and $d_{100} = 4.5$ Å.

We thus come to the conclusion that the DPPA and C20 molecules are oriented normal to the substrate while the hydrocarbon chains are forming a triangular lattice. For these two lipids the areas per lipid molecule obtained from the lattice constants agree well with the monolayer data (cf. Table I). These areas corresponds nearly to a tight packing of the chains which provides evidence that the molecules are oriented normal to the surface both on the air/water interface and on the substrate.
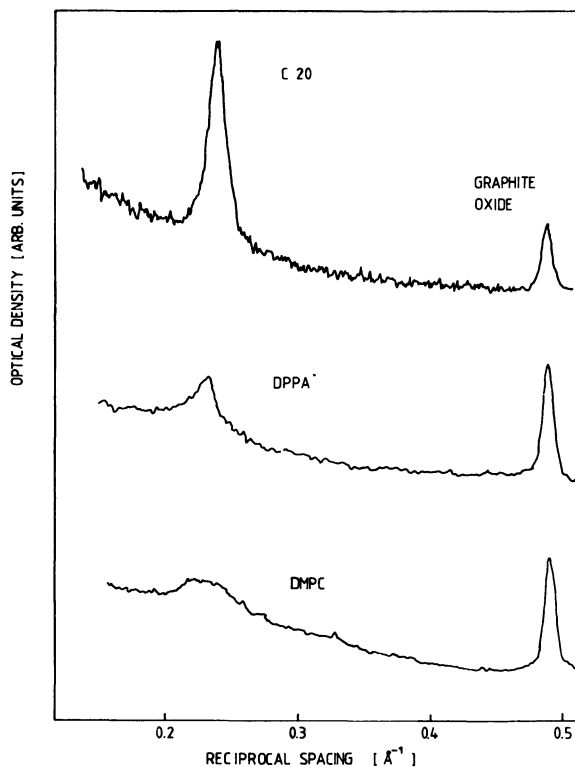

Fig. 10. — Densitometric evaluation of diffraction pattern of monolayers of several lipids deposited on graphite oxide. The right side bands are from graphite oxide and the left peaks are the (100) monolayer reflections. All monolayer reflections. All monolayers were transferred from region IV.

Table I. — *Results of densitometric evaluation of electron diffraction pattern of monolayers transferred from high pressure* (30 mN/m, $\pi > \pi_c$) *onto graphite oxide. The half width of graphite oxide is* 0.008 Å^{-1}.

Lipid	DMPC	DPPA	C20
d_{100}	4.4	4.3	4.2
Area per chain Å^2	22.3	21.3	20.3
Area per chain from filmbalance Å^2	22.5	21.3	20.3
Half width of reflexes in Å^{-1}	0.040	0.016	0.014

The situation is more complicated for the lecithins. According to references [1, 4, 10] the area per molecule on air/water varies between 40 Å^2 and 45 Å^2. The average lattice constant of $d_{100} = 4.4$ Å leads to a value of 45 Å^2. Obviously the chains are tilted both on air/water and on the substrate. The apparent splitting

of the reflections in the radial direction may be explained by assuming that the lipid chains form an ortho-rhombic net [20] in order to achieve an equal interchain distance. Due to the large angular width of the reflections a more detailed structure determination is not possible.

There may be a slight structural change if the monolayer is transferred to the solid substrate since all lecithins studied. (DMPC, DPPC, DSPC) exhibit the same spider's web of narrow cracks if they are transferred from the high pressure phase IV. This pattern of cracks is shown in figure 11 at low magnification. It is seen that they often follow the crystal planes of a hexagonal lattice. The cracks may run over distances of some μm in one direction. However, they also originate and end within the monolayer. This strongly suggests that they are caused by an internal contraction of the monolayer during the deposition process and not by a desintegration of the monolayer due to a sudden drop in the lateral pressure upon the transfer. The latter effect would lead to broad cracks (cf. Fig. 4a). This contraction could also explain the somewhat smaller values of the area per molecule obtained for the films on solid substrates as compared with the mono-layer value of 48 Å of reference [1].

4.1.2 *Condensed phase* (III) *and on the nature of the transition at π_c.* — In the intermediate condensed state (III) the transferred film consists of homogeneous platelets in all cases studied. These may be loosely connected by disordered material of a grainy appearance as in the case of DPPA (cf. Fig. 4a), they may be separated by material free cracks as in the case of DPPC (cf. Fig. 6b) or they may be completely separated as visible in figure 2c. The platelets have an irregular shape and the shadowing experiments show that they have a thickness of about 25 Å and thus consists of monolayers. Remarkably, the platelets of both the phosphatidylcholines and of DPPA exhibit small holes of 100-500 Å diameter. The diffraction patterns consist of rings of relative high intensity. The width of the intensity profile in the radial direction is about equal to that of the corresponding reflection of the high pressure crystalline phase.

The above finding of large platelets in the case of the monolayer transfer from the intermediate pressure region together with the observation of relatively sharp diffraction rings provide strong evidence that the monolayer state III is a crystalline phase. We thus conclude as in our previous work [1] that the transition at π_m (called main transition in reference [1]) is accompanied by a symmetry break. It is quite unlikely that the formation of crystal platelets with diameters of the order of 1 μm can take place during the film transfer.

The breaks in the isotherms at π_c [1] has some typical features of a 2nd order transition and for that reason it was tentatively attributed to a symmetry-breaking transition at which the hydrocarbon chains go over from a tilted to a non-tilted orientation [1]. Such a transition could not be verified in the present experi-
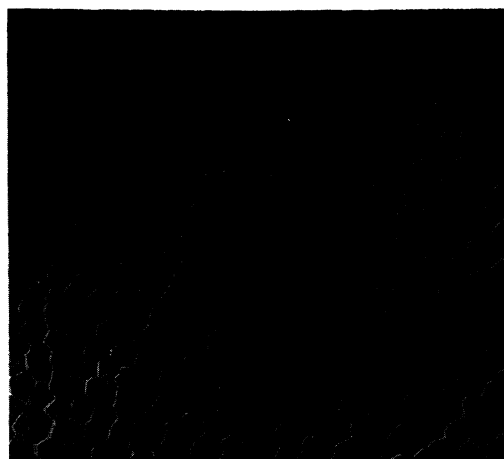

Fig. 11. — Low magnification of non-shadowed but stained distearoylphosphatidylcholine (DSPC) monolayer taken by the low magnification phase contrast technique (π = 30 mN/m, 20 °C).

ment. The appearance of holes and small pieces of monolayer observed if DMPC (Fig. 7b) or DPPA (Fig. 4b) are transferred from state III could in principle be attributed to a change from a tilted to a non-tilted (or less tilted) state which would lead to a lateral contraction. On the other side the holes and loosely packed small aggregates could also be explained in terms of the coexistence of crystalline and fluid phases in state III. The small crystallites (cf. Fig. 4b) could well be attributed to fluid patches at the air/water interface which condense into monolayer crystallites during transfer. The holes could also be caused by the condensation of fluid phase upon transfer. According to figure 8b small crystalline pieces are indeed formed if a monolayer is transferred from the fluid phase. An interpretation of state III in terms of a fluid-solid coexistence has been given by Tscharner and McConnell [3]. Thus it cannot be excluded that states III and II are actually identical. The only difference is that in state III most of the lipid is in the crystalline state. This is certainly the case for the lecithins since according to figure 7b, the transferred monolayer exhibits the same spider's web of cracks as the completely condensed phase IV. The only difference is the appearance of the small holes within the platelets and the diffuse rims of these.

In this picture, the break at π_c could be interpreted in terms of a merging of randomly oriented crystalline platelets into a single crystal monolayer. This process is associated with a reorientation of the platelets because merging is only possible if the orientation of crystal planes of adjacent platelets are matched [27]. Moreover, one has to overcome the line tension at the boundaries of the platelets which could well account for the relatively high transition pressure π_c.

4.1.3 *Low pressure states* ($\pi \leqslant \pi_m$). — According to figure 8a small interconnected islands are formed if the monolayer is transferred from $\pi = \pi_m$. The islands

are interrupted by patches which seem to be free of material. The free area amounts to about 20 % of the total surface. The electron diffraction pattern exhibits a weak but sharp ring and the islands thus have to be in a crystalline state. The average coherence length of these solid domains is about 250 Å. It is very likely that they exist already on the air/water interface although they may have become somewhat enlarged during the transfer. As shown in figure 8b the islands are indeed considerably smaller and the free area amounts to about 30 % if the film is transferred from a pressure just below the beginning of the phase transition.

Our results therefore strongly suggest that region II/III corresponds to the coexistence of fluid and crystalline domains with coherence length of some 100 Å. This provides strong experimental evidence for our previous interpretation of the finite slope of the main transition at π_m [1]. We had postulated that it can be explained in terms of the melting (or crystallization) of small cooperative units comprising some 100 molecules (cf. Table 1 of [1]). Very recently Georgallas and Pink [21] presented a theory based on Monte Carlo simulations where they showed that the finite size of the slope comes about because of the finite size of the cooperatively melting domains. It thus appears that the film transfer experiment can give information about the state of the film on the air/water interface.

4.2 ON THE VISCOSITY OF THE INTERMEDIATE PRESSURE REGION III. — According to fluidity measurements by several groups [22-26] both fatty acid and phospholipid monolayers in state III exhibit a low, fluid-like viscosity. Measurements of the rate of monolayer flow (driven by a lateral pressure difference) [11] show that the viscosity of DPPC decreases by some two orders of magnitude if the pressure is increased above π_c while the viscosity of state III is essentially the same as in the fluid state. According to Jarvis [22] the surface viscosity of fatty acids decreases continuously from a low value characteristic for fluid monolayers (Point M′ of Fig. 1) to a solid-like value (at $\pi = \pi_c$) that is just within region III of figure 1. The same holds for measurements of Hayashi et al. [25]. The latter workers obtained a sharp rise in viscosity with increasing pressure just at the end of the main transition (M′ of Fig. 1).

The high softness of the monolayers in state III is not necessarily an unambiguous indication of a fluid state. Thus, the coexistence of a fluid and solid phase would certainly lead to a fluid-like macroscopic viscosity. Moreover, if the condensed state would only consist of a mosaic-like arrangement of platelets of solid monolayers one could well expect a low shearing strength. This is just the type of structure observed in the intermediate pressure region as is shown for instance for the case of DPPA in figure 4a. Such a two-dimensional mosaic-structure is expected to behave analogous to a normal powder which may have a fluid-like shearing strength.

Recent elegant measurements of lateral diffusion in phospholipid monolayers [26] confirm this interpretation. It is found that the lateral diffusion coefficient of phospholipid analogs decreases sharply from a value characteristics for fluid phases to a value typical for crystalline phases within the region of the main transition.

4.3 ON THE LONG-RANGE ORDER OF THE CRYSTALLINE MONOLAYERS. — The appearance of sharp reflections (sometimes in hexagonal array) clearly shows that the monolayer at state IV exhibits long-range crystalline order at least with respect to the orientation of the crystal planes. However, according to the densitometric analysis, the density profiles in the radial direction are by a factor of 5 to 10 (cf. Table I) broader for monolayer than for normal crystals such as graphite oxide. The radial density profiles I have the appearance of Lorentzian shapes at least for DPPA and C20

$$I(\mathbf{q}) \propto \frac{1}{1 + \xi^2(\mathbf{q} - \mathbf{q}_0)^2}$$

where $\mathbf{q}$ is the scattering vector and ξ the half width. Since the electron beam is directed parallel to the normal of the monolayer and since the hydrocarbon chains are not tilted, the scattering vector is determined by the components q_x, q_y in the monolayer plane alone. Thus ξ is a correlation length which measures the range of the positional order of the hydrocarbon chains. The width of the spots in the angular direction is a measure of the disorder in the crystal plane orientation. The analysis yields correlation lengths of 70 Å for C20 and 60 Å for DPPA. There are three possible explanations for the broadening of the Bragg reflections. First it may be due to instrumental artefacts or to a tilted substrate with respect to the electron beam direction.

This may be excluded since the graphite oxide substrate shows sharp reflections. Secondly, the broadening may be due to normal mosaic spread. The diameter of the two-dimensional crystallites is 1 μm so that this possibility may be excluded as well. This provides some evidence that the radial broadening is due to a reduced positional long range order, characterizing the arrangement of the chains in the plane of the monolayer. The observed angular width is certainly determined by the spread in the orientation of the crystal-platelets. This may be large since the narrow cracks allow some rotational freedom of the platelets about axes normal to the monolayer surface. It is thus well probable that the solid monolayers exhibit long range bond orientational order but short range positional order [28]. The same type of structure has been reported for certain smectic phases such as the smectic F-phase of TBPA [29, 30].

Acknowledgments.

References

[1] ALBRECHT, O., GRULER, H. and SACKMANN, E., J. Physique 39 (1978) 301.

[2] MONTAL, M., DARSZON, A. and SCHINDLER, H., Quart. Rev. Biophys. 14 (1981) 1.

[3] TSCHARNER, V. and McCONNEL, H. M., Biophys. J. 36 (1981) 56.

[4] CADENHEAD, D. A., MÜLLER-LANDAU, F. and KELLNER, B. M. J. in Ordering in two-dimensions, Sinha, S.K. ed. (Elsevier-North Holland (Biomedical Press) Amsterdam) 1980, p. 73-81.

[5] PERSHAN, P., Physics Today 35 (1982) 34.

[6] ROBERTS, G. G., Springer Series in Electrophysics 7 (1981) 56.

[7] SWALEN, J. D., TACKE, M., SANTO, R., RIECKHOFF, K. E. and FISCHER, J., Helvetica Chimica Acta 61 (1978) 960.

[8] GROS, L., RINGSDORF, H. and SCHUPP, H., Angew. Chem. 93 (1981) 311.

[9] ALBRECHT, O., JOHNSTON, D. S., VILLAVERDE, C. and CHAPMAN, D., Biochim. Biophys. Acta 687 (1982) 165.

[10] PHILLIPS, M. C., WILLIAMS, R. M. and CHAPMAN, D., Chem. Phys. Lipids 3 (1969) 234.

[11] LÖESCHE, M., MÖHWALD, H. and SACKMANN, E., to be published.

[12] FORMANEK, H., Ultramicroscopy 4 (1979) 227.

[13] BAUMEISTER, W., HAHN, M., in : Principles and Techniques of Electron Microscopy, M. A. Hayat ed. (Van Nostrand Reinhold Comp. New York) 1978, p. 4.

[14] ARCIDIANACONO, A., STASIAK, A. and KOLLER Th., 9th International Congress on Electron Microscopy (North Holland Publ. Comp.) 1980.

[15] LANGMORE, J. P., WALL, J. and ISAACSON, M. S., Optik 38 (1973) 335.

[16] RIEKE, W. D. Optik 19 (1962) 81.

[17] RIES, H. E., WALKER, D. C., J. Colloid Sci. 16 (1961) 361.

[18] SHEPPARD, E., BRONSON, R. P. and TCHEUVEKDJIAN, N., J. Colloid Sci. 20 (1965) 755.

[19] RUOCCO, M. and SHIPLEY, G. G., Biochim. Biophys. Acta 684 (1982) 59.

[20] HUI, S. W., Chem. Phys. Lipids 16 (1976) 9.

[21] GEORGALLAS, A. and PINK, D. A., Can. J. Phys. 60 (1982) 1678.

[22] JARVIS, N. J., J. Phys. Chem. 69 (1965) 1789.

[23] ADAM, N. K., The Physics and Chemistry of Surfaces, 3red (Oxford Univ. Press) 1941.

[24] ADAMSON, A. W., Physical Chemistry of Surfaces, 3rd ed. (John Wiley and Sons) 1976.

[25] HOYASHI, M., MURAMATSU, T., HARA, I. and SEIMIYA, T., Chem. Phys. Lipids 15 (1975) 209.

[26] PETERS, R., to appear in EMBO Journal (1983).

[27] LANDAU, L. D., Collected Papers of Landau, D. Ter Haar ed. (Pergamon Press) 1965, p. 540.

[28] NELSON, D.R. and HALPERIN, B. I., Phys. Rev. B 19 (1979) 2457.

[29] GANE, P. A. C., LEADBETTER, A. J., BENATTER, J. J., MOUSSA, F. and LAMBERT, M., Phys. Rev. A 24 (1981) 2694.

[30] LITSTER, J. D., Liquid Crystal of One and Two-Dimensional Order, W. Helfrich and G. Heppke ed. (Springer Verlag, Berlin) 1980.